MODELING POWDERED SORBENT INJECTION IN COMBINATION WITH FABRIC FILTER FOR THE CONTROL OF MERCURY EMISSIONS

Joseph R. V. Flora
Department of Civil and Environmental Engineering
University of South Carolina, Columbia, SC 29208

Richard A. Hargis, William J. O'Dowd, Henry W. Pennline
National Energy Technology Laboratory, U.S. Department of Energy
P.O. Box, 10940, Pittsburgh, PA 15236

Radisav D. Vidic*
Department of Civil and Environmental Engineering
University of Pittsburgh, Pittsburgh, PA 15261

ABSTRACT

A two-stage mathematical model for mercury removal using powdered activated carbon injection upstream of a baghouse filter was developed, with the first stage accounting for removal in the ductwork and the second stage accounting for additional removal due to the retention of carbon particles on the filter. This model incorporates key mass transfer and equilibrium processes that govern adsorption of mercury vapors on activated carbon in the duct and on the fabric filter. Most of the kinetic parameters were estimated from literature correlations and manufacturers specifications, while adsorption equilibrium parameters were determined by fitting the model to a set of experimental data obtained from a pilot-scale coal combustor system. Predictive capability of the model was demonstrated using experimental measurements on the same pilot-scale system. The model shows that removal in the ductwork is minimal, and the additional carbon detention time from the entrapment of the carbon particles in the fabric filter enhances the mercury removal from the gas phase. A sensitivity analysis on the model shows that mercury removal is dependent on the isotherm parameters, the carbon pore radius and tortuosity, the carbon to mercury ratio, and the carbon particle radius.

INTRODUCTION

Mercury control models represent a combination of the microscale models that account for the kinetics of the adsorption process on the adsorbent particle and macroscale processes that account for the mass balance in the reactor system used to control gaseous emissions. Microscale models typically include the external (film) resistance to transport and internal transport inside the sorbent particle. External resistance to transport is usually modeled according to Fick's first law of diffusion while intraparticle transport can be broadly classified in the following categories: (a) pore diffusion, (b) surface diffusion, and (c) dual pore and surface diffusion.

Chen and co-workers[1-2] developed one of the first and simplest mercury control models. Their model describes mercury removal by powdered sorbent injected into the flue gas duct but did not account for the impact of particulate control devices used later in the process (i.e., electrostatic precipitator or fabric filter). The authors assumed that all mercury molecules that diffuse across the external film are completely captured by the sorbent particle. External resistance to mass transfer was modeled by Fick's first law assuming negligible concentration of mercury on the external surface of the adsorbent particle. These authors also offered a simplified solution to the transport equation inside the sorbent particle (assuming the small uptake of adsorbate relative to the total amount of adsorbate in the batch reactor).

Flora et al.[3] developed a model for a closed batch reactor system that accounted for both external mass transfer resistance and intraparticle transport. External mass transfer was modeled using Fick's first law, while the intraparticle transport was modeled using the surface diffusion transport mechanism. They used the model to estimate equilibrium (Langmuir isotherm) and kinetic parameters (D_s and k_f) from closed-batch mercury uptake experiments, and developed simple design nomograms for 80 and 90% mercury removal in the duct. One of the major drawbacks of this study is that the kinetic and adsorption parameters were obtained from experimental data that were collected using pure nitrogen as a carrier gas. Thus, the parameters of their model do not account for the effect of other chemical reactions that may be catalyzed by the carbon surface in the presence of reactive gases that are typical for coal-fired power plants. In addition, the experimental data were obtained using unreasonably high mercury concentration because of the inherent limitations of the analytical procedures used to measure mercury concentrations in the gas phase.

Meserole et al.[4] extended the model of Chen and co-workers[1-2] in order to account for the additional mercury removal that is encountered as a result of the extended contact time between the sorbent particle and mercury on the fabric filter. Mercury removal in the duct was assumed to be external mass transfer limited and the model did not incorporate any terms to account for intraparticle diffusion. Additional mercury removal on the fabric filter was modeled using the fixed-bed reactor model coupled with an external mass transfer limited diffusion model. Adsorption equilibrium parameters for the Freundlich isotherm were obtained by fitting the model to breakthrough curves obtained from fixed-bed laboratory-scale experiments with simulated flue gas. These parameters were subsequently used to assess mercury removal in the duct and evaluate the impact of mercury concentration and particle size on the removal efficiency. Mercury removal on the fabric filter was modeled using the prediction from a fixed-bed reactor model that assumed a bed thickness corresponding to a 45 minute accumulation time and complete cleaning of the fabric filter after that period.

Serre et al.[5] used the same external mass transfer model as Chen and co-workers[1-2] to asses the largest sorbent particle size that would reduce the effect of external mass transfer resistance on mercury uptake in the entrained-flow reactor. They suggested that the particle size of 14 μm or less would be sufficient to minimize external mass transfer effects.

Recently, Scala[6-7] developed a model describing mercury removal via carbon adsorption in the duct and on the carbon entrained in a fabric filter. To our knowledge, this was the first model

that addresses the moving boundary problem associated with a growing adsorbent layer on a filter bed.

The objective of this study was to develop a model that describes mercury removal using activated carbon in a baghouse filter. First, the model development is described and a sensitivity analysis is performed to evaluate the parameters that impact the calculated mercury removal from the system. Second, model parameters were estimated using a subset of the data collected from a pilot-scale system and the model predictions are verified using the rest of the data from the same system.

MATHEMATICAL MODEL

A two-stage model describing mercury removal from the gas phase by activated carbon injection and subsequent deposition and removal in a baghouse filter is developed using the pore diffusion model (PDM) to describe the kinetics of adsorption of mercury from the carbon surface into the activated carbon particle. The first stage involves coupling the PDM to a model for a plug flow system to describe mercury uptake in the ductwork, while the second stage involves coupling the PDM to a model for a packed-bed. In the second stage, the growth and deposition of the activated carbon particles on the baghouse filter is incorporated in the model to account for additional mercury uptake of the particles due to an increased detention time in the system. Detailed description of governing equations that describe mercury adsorption in the duct and on the baghouse filter is given elsewhere[8] and will not be repeated here. For mercury removal in the duct, governing equations were reduced to ordinary differential equations using orthogonal collocation methods[9] with 5 interior collocation points in the activated carbon particle. The resulting system of equations was solved using DDASSL[10], a subroutine capable of solving algebraic and ordinary differential equations simultaneously.

For the second stage, the length of the packed-bed varies with time and this moving boundary problem was addressed by using the appropriate coordinate transformation.[8,11] The final model equations for the second stage were also reduced to ordinary differential equations using orthogonal collocation methods[9] with 5 interior collocation points in the activated carbon particle and 7 interior collocation points in the packed bed. The resulting system of equations was solved using DDASSL[10].

Parameter Estimation

The following equation was used to calculate the pore diffusion coefficient[12],

$$D_p = \frac{\varepsilon_p}{\tau_p}\left(\frac{1}{D_{Hg}} + \frac{1}{D_{Kn}}\right)^{-1} \quad (1)$$

where the diffusivity of mercury in the gas phase was estimated from the Chapman-Enskog theory[13], and the Knudsen diffusion coefficient was calculated using[14]

$$D_{Kn} = 9700\frac{d_{pore}}{2}\left(\frac{T_k}{MW_{Hg}}\right)^{1/2} \quad (2)$$

The mass transfer coefficient in the duct was estimated using the following empirical correlation for forced convection around a solid sphere[13],

$$\frac{2k_f r_p}{D_{Hg}} = 2.0 + 0.6\left(\frac{2r_p v_o}{\nu}\right)^{1/2}\left(\frac{\nu}{D_{Hg}}\right)^{1/3} \quad (3)$$

The relative velocity (v_o) between the activated carbon particles and the gas stream was estimated using Stoke's Law with Cunningham's correction.[15] The mass transfer coefficient in the baghouse filter was estimated using the following empirical correlation for a packed-bed[16]

$$\frac{2k_f r_p}{D_{Hg}} = 2.0 + 1.1\left(\frac{2r_p v\varepsilon_b}{\nu}\right)^{0.6}\left(\frac{\nu}{D_{Hg}}\right)^{1/3} \quad (4)$$

Equation (4) intrinsically account for the effects of dispersion in the packed bed, which is calculated from[16]

$$D = \frac{20}{\varepsilon_b} D_{Hg} + v r_p \quad (5)$$

Physical characteristics of Norit Darco FGD carbon were used in the parameterization of the model. The median pore diameter was reported to be 150 Angstroms[17] and was used in estimating D_{Kn}. The activated carbon density (ρ_p=2.04 g/cm^3) and porosity (ε_p=0.67) were provided by the manufacturer. Yang[18] reports that the tortuosity (τ_p) for activated carbons ranges from 5 to 65, and Bush et al.[19] reports that the bed porosity (ε_b) for full-scale coal-fired power plants employing a baghouse for particulate control ranges from 0.57 to 0.86.

Sensitivity Analysis

Table 1 lists baseline model parameters that were used in this study. It is important to note that these parameters were not arbitrarily chosen but that they reflect realistic conditions in powdered sorbent injection systems. For example, isotherm parameters listed in Table 1 correspond to the parameters that were obtained for the experimentally measured mercury removals at 275 °F as will be discussed later in this manuscript together with details for other parameters listed in Table 1.

Figure 1 shows the predicted removal that can be accomplished in the duct for a 2 second contact time as well as the removal of mercury from the section of the baghouse filter that is equal to one-tenth of the total filter area and overall mercury removal in the baghouse using the hypothetical base case scenario shown in Table 1. The removal of mercury in the ductwork is limited by mass transfer from the bulk flue gas to the adsorbent particle and is relatively small (~2-3 %) for a 2 second flight time. As the carbon particles are retained on the filter, the additional detention time allows the carbon particles to remove more mercury from the flue gas. This is shown by the increase in fractional removal with time from the section that is comprised of the one-tenth of the total filter area. Cleaning this section of the filter after 15000 seconds results in the complete removal of the accumulated adsorbent and subsequent reduction in the fractional removal to the levels equal to those at the exit from the ductwork. If one-tenth of the total filter area is cleaned every 1500 seconds, then different sections of the filter are removing mercury at different levels depending on the depth of the accumulated adsorbent bed at that section. The overall mercury removal is thus a composite average of the removal in different sections of the fabric filter a nd the profile of mercury removal will have a jagged nature due to

Table 1. Base case scenario for the model.

Varied Parameters	
Langmuir isotherm parameter, q_{max}	3020 μg/g
Langmuir isotherm parameter, b	3.9 $m^3/\mu g$
Influent mercury concentration, c_o	5 $\mu g/m^3$
Flue gas flow rate, Q	1 m^3/s
Carbon injection rate, $\dot{m}_c$	0.025 g/s
Sorbent particle radius, r_p	0.0015 cm
Sorbent average pore diameter, d_p	150 Angstroms
Tortuosity, τ_p	5
Filter bed porosity, ε_b	0.7
Sorbent porosity in the bed, ε_{cb}	0.005
Time in duct	2 s
Cleaning cycle interval	1500 s
Fraction of filter cleaned per cycle	0.1
Fixed Parameters	
Temperature, T	275°F
Sorbent particle density, ρ_p	2.04 g/cm^3
Sorbent particle porosity, ε_p	0.67
Area of the baghouse filter, A	50 m^2

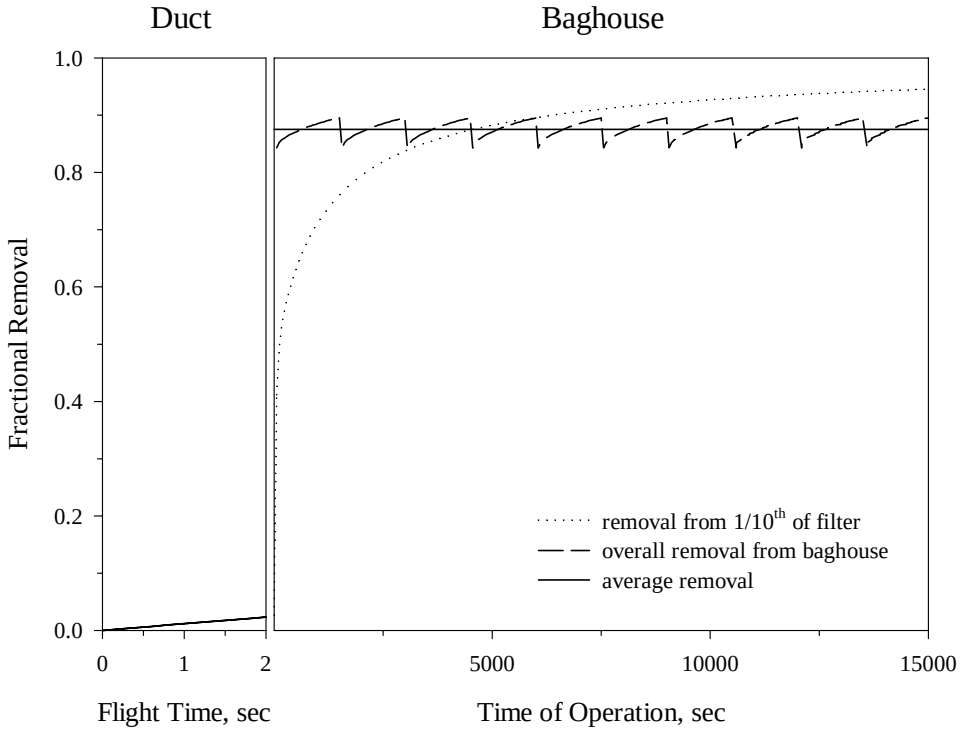

Figure 1. Dynamic profile of mercury removal from a $1/10^{th}$ section of the baghouse filter and from the overall baghouse filter system

the intermittent partial cleaning of the filter. The overall removal never decreases to the levels equal to those at the exit from the ductwork and the average mercury removal efficiency under the base conditions shown in Table 1 is 87.5%.

Because experiments can often be resource-intensive, a model's ability to estimate the process performance due to a change in an operating condition can be invaluable. Furthermore, it is also necessary to understand changes in the model predictions due to uncertainties in the process variables. Thus, the sensitivity of the model predictions (i.e., the average mercury removal) as a function of various parameters is performed and is compared to the hypothetical base case shown in Table 1. It is important to note that the sensitivity analysis for the most important parameters is reported here while a more complete evaluation can be found elsewhere[8]. The impact of isotherm parameters on mercury removal efficiency from the baghouse is shown in Figure 2. Higher values of b (hence higher forward rates of adsorption relative to desorption) resulted in higher removal efficiency. However, varying b over two orders of magnitude only slightly impacted the removal efficiency relative to the base conditions. Increasing q_{max} had a more significant impact on the removal efficiency. This would indicate that using carbons with higher adsorptive capacity could be beneficial assuming all other parameters and process conditions are similar. At high values of q_{max} and b, the isotherm tends towards a constant isotherm and the fractional removal converges towards a constant value where the percent removal is governed by mass transfer.

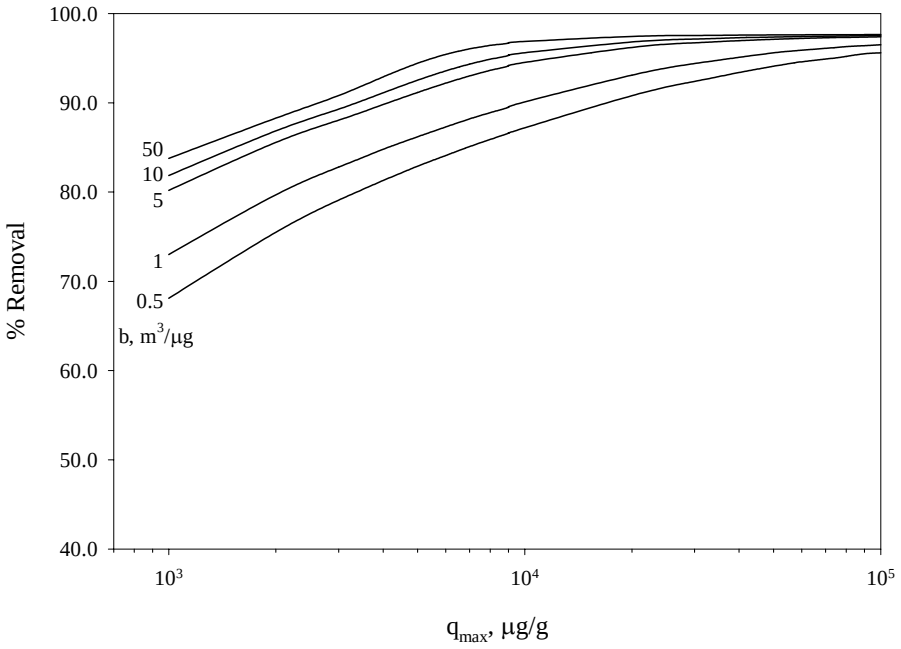

Figure 2. The effects of the isotherm parameters on the calculated average mercury removal efficiency from the baghouse filter

The impact of carbon injection rate will be discussed in Model Calibration and Verification section later in the text.

The size of carbon particles injected upstream of the baghouse filter is another process parameter that can potentially be varied to control mercury removal efficiency. Under the

base conditions and in the range of reasonable carbon particle radii, using smaller carbon particles will enhance the rate of mercury mass transfer from the bulk solution to the particle and result in better mercury removal from the baghouse filter (Figure 3). Figure 3 also demonstrates that uncertainty in bed porosity will not significantly impact predicted mercury removal efficiency from the baghouse filter.

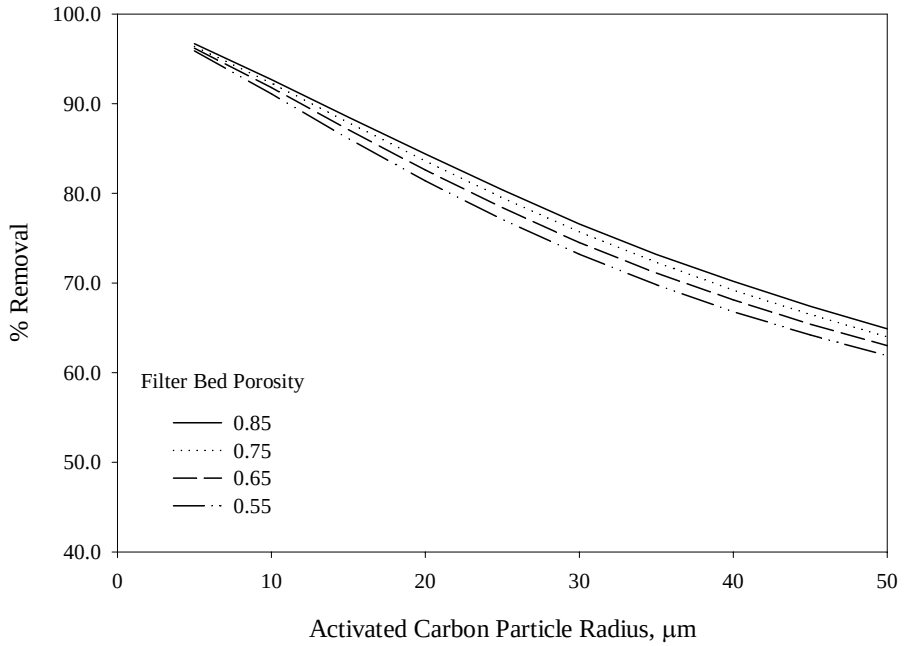

Figure 3. The effects of the activated carbon particle radius and the filter bed porosity on the calculated average mercury removal efficiency from the baghouse filter

Figure 4 shows that the pore diameter and tortuosity significantly impacts the predicted mercury removal efficiency from the baghouse filter. These parameters are used in the calculation of the pore diffusion coefficient (Equations (1) and (2)). An increase in the pore diameter increases the Knudsen diffusivity, which increases the pore diffusion coefficient. Larger pore diameters allow mercury to diffuse more freely into the pores, thereby increasing the intraparticle mass transfer rates and effectively removing more mercury from the bulk. In contrast, an increase in tortuosity means that mercury molecules must travel a longer distance as they diffuse from the activated carbon surface into the particle. The resulting decrease in the pore diffusion coefficient decreases the intraparticle mass transfer rate and reduces the mercury removal efficiency.

MODEL CALIBRATION AND VERIFICATION

The model was calibrated and validated against the results obtained from a pilot-scale system. The 500-lb/hr furnace system used in this study consists of a wall-fired pulverized coal furnace equipped with a water cooled convection section, a recuperative air heater, spray dryer, baghouse, and associated ancillary equipment (fin-fan coolers, surge tanks, coal hoppers, blowers, pumps, etc). Detailed description of the pilot-scale unit and experimental conditions used int his study are reported elsewhere[20,21] and will not be repeated here.

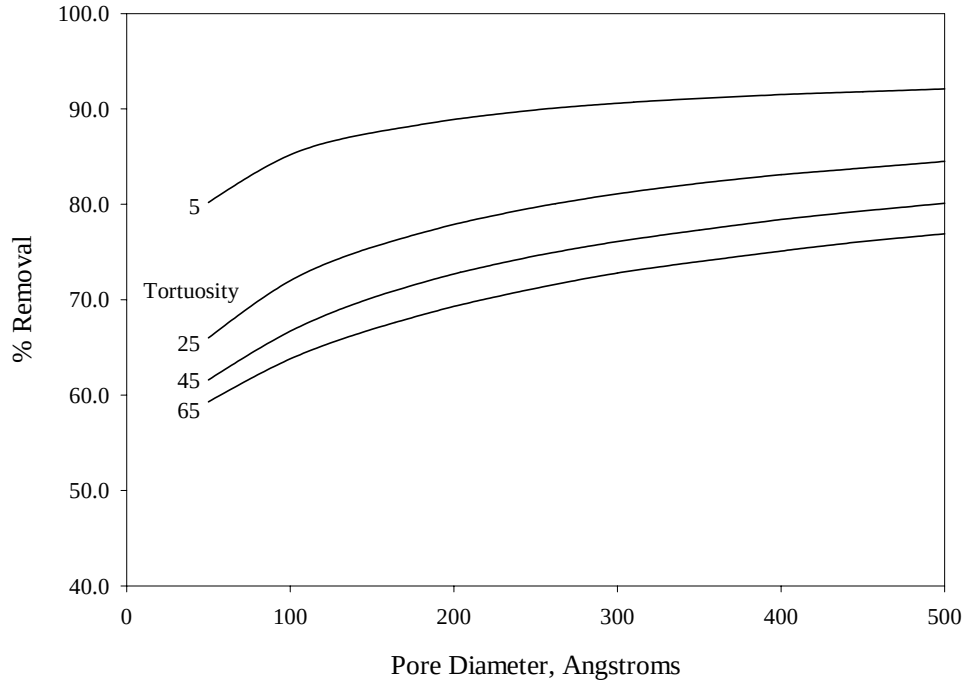

Figure 4. The effects of the pore diameter and tortuosity in the activated carbon particles on the calculated average mercury removal efficiency from the baghouse filter

All mercury removals and material balances were calculated from flue gas measurements using either EPA Method 101A[22] for total mercury or the Draft ASTM Method[23], also known as the Ontario-Hydro (O-H) method, for total and speciated mercury. These wet-chemical methods have been found to give good, repeatable results on this unit[20,21].

Model Calibration

Table 2 shows the results of pilot-scale tests, including the average temperature in the system, influent mercury concentration, flue gas flow rate, activated carbon injection rate, and average mercury removal in the system. It is important to note that mercury concentrations and removal efficiencies reported in this table represent steady-state results based on the two-hour average sampling period that is required for the O-H method. Mercury mass balances around the baghouse ranged from 77 to 136% while the mass balance around the entire system averages 83%[20].

Carbon to mercury (C/Hg) ratios of up to 16,300 (g/g) were tested in this study and mercury removal ranged from negligible to above 90%. As expected, mercury removal at a particular baghouse temperature increases with increasing sorbent-to-mercury ratio. Also, mercury removal efficiency increases with decreasing baghouse temperature for a constant injection ratio. Data sets 1 and 23 and 5 and 17 showed about 10 and 30% mercury removal, simultaneously to the data sets in the pilot scale studies. The sum of the squares of the differences between the average removal predicted by the model and the data sets was minimized by varying q_{max} and b within a simulated annealing algorithm[24].

Table 2. Mercury Removal from the Pilot-Scale Tests.

Data Set	Temp., °F	Influent Mercury, $\mu g/m^3$	Flow Rate, m^3/s	AC Injection Rate, g/s	Time In Flight, s	Percent Mercury Removal
1	294	2.86	1.47	0.0000	N/A	12.2
2	294	2.76	1.53	0.0485	2	84.1
3	265	3.01	1.50	0.0538	2	88.7
4	268	3.05	1.41	0.0288	2	68.2
5	296	2.94	1.46	0.0000	N/A	31.0
6	296	3.11	1.49	0.0131	2	42.8
7	296	2.94	1.58	0.0276	2	65.6
8	270	3.30	1.48	0.0144	2	62.7
9	275	2.96	1.20	0.0071	2	(3.7)
10	306	2.96	1.27	0.0081	2	(5.4)
11	244	3.31	1.08	0.0267	2	90.0
12	250	2.32	1.05	0.0147	2	87.5
13	250	2.06	1.10	0.0149	2	79.6
14	200	2.26	1.08	0.0149	2	96.5
15	262	5.31	1.00	0.0146	0.5	80.8
16	301	4.25	1.05	0.0271	0.5	73.2
17	264	5.36	0.92	0.0000	N/A	32.8
18	271	4.24	0.97	0.0542	0.5	96.7
19	271	4.14	1.00	0.0551	2	92.5
20	272	3.77	1.01	0.0621	0.5	91.8
21	272	4.24	0.99	0.0294	0.5	87.7
22	271	4.43	0.93	0.0290	2	86.2
23	270	4.41	0.95	0.0000	N/A	10.2

Three data sets within a reasonably close temperature range were used to obtain q_{max} and b from the experiments. Table 3 shows the data sets used and the corresponding values for the isotherm constants, while Figure 5 shows the model fits to the Data Group 1 based on the parameters shown in Table 1. The jagged nature of the model fit is due to the intermittent cleaning of the baghouse, with the intermittent drop in the fractional removal indicating when the baghouse was cleaned. Different data sets had different cleaning intervals. In all the data sets, it was assumed that $1/9^{th}$ of the total filter area in the baghouse was cleaned in each cleaning cycle. The average removal from the pilot test is also plotted in the figure. Mercury sampling from the pilot tests were not collected with a small enough frequency to clearly show the jagged nature predicted by the model. Similar results were obtained for Data Groups 2 and 3.

The model shows that the removal of mercury in the ductwork is minimal. The immediate increase in the removal efficiency after the ductwork is a result of the contribution of the various fractions of the baghouse filter in mercury removal. The fraction of the filter that was just cleaned would have low removal efficiency because the filter cake had not yet been formed, while the fraction of the filter with a relatively mature filter cake would already be

effectively removing mercury from the flue gas. The resulting composite average contribution of all the fractions of the bed to the mercury removal efficiency is plotted in Figure 5.

Table 3. Isotherm constants obtained at different temperatures.

Data Group	Average Temperature, °F	Data Sets	q_{max}, μg/g	b, $m^3/\mu g$
1	248	11, 12, 13	70714	0.107
2	271	8, 19, 22	2909	7.02
3	295	2, 6, 7	496	20

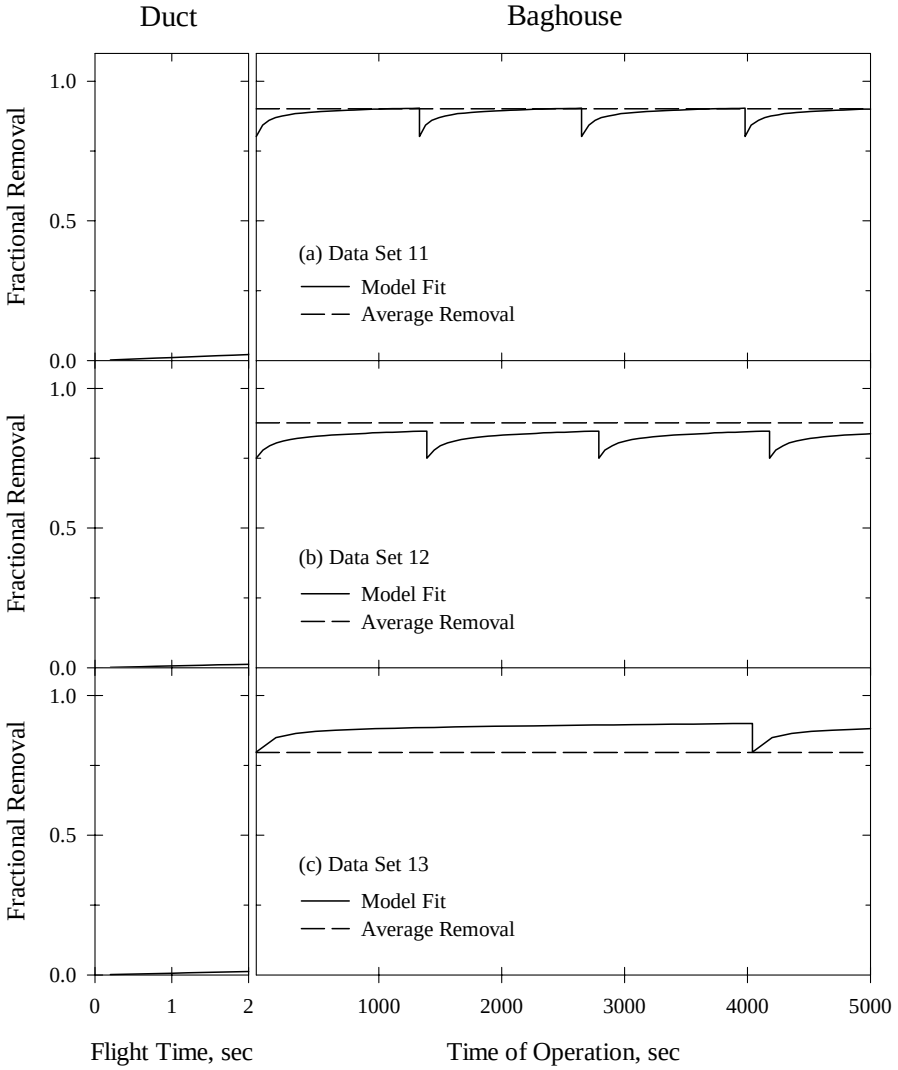

Figure 5. Average mercury removal and model fit for (a) Data Set 11, (b) Data Set 12, and (c) Data Set 13

The isotherm parameters and an Arrhenius relationship describing the variation of these parameters with temperature are shown in Figure 6. An increase in temperature results in a lower capacity of the carbon for mercury, which is characteristic of an exothermic adsorption

process and is consistent with earlier findings. The Langmuir coefficient, b, increased with temperature. As reasoned in an earlier study[3], this coefficient can be conceptualized as the ratio of the kinetic coefficient for adsorption to the kinetic coefficient for desorption. It is possible that with an increase in temperature, the kinetic coefficient for adsorption increased but the kinetic coefficient for desorption did not increase with the same magnitude. A shift in the adsorption mechanism from physical to chemical at a higher temperature could also result in a proportionately lower increase in the desorption kinetic coefficient[25]. Similar variations in the isotherm coefficients with temperature have been reported for different adsorbents[26,27]. At a temperature of 135°C (275°F) and mercury concentration of 59 μg/m^3, Hsi et al.[17] reported the capacity of Norit Darco FGD of 2566 μg/g, which is reasonably close (within 17%) to the capacity calculated for that temperature using the data in Figure 6 (3007 μg/g).

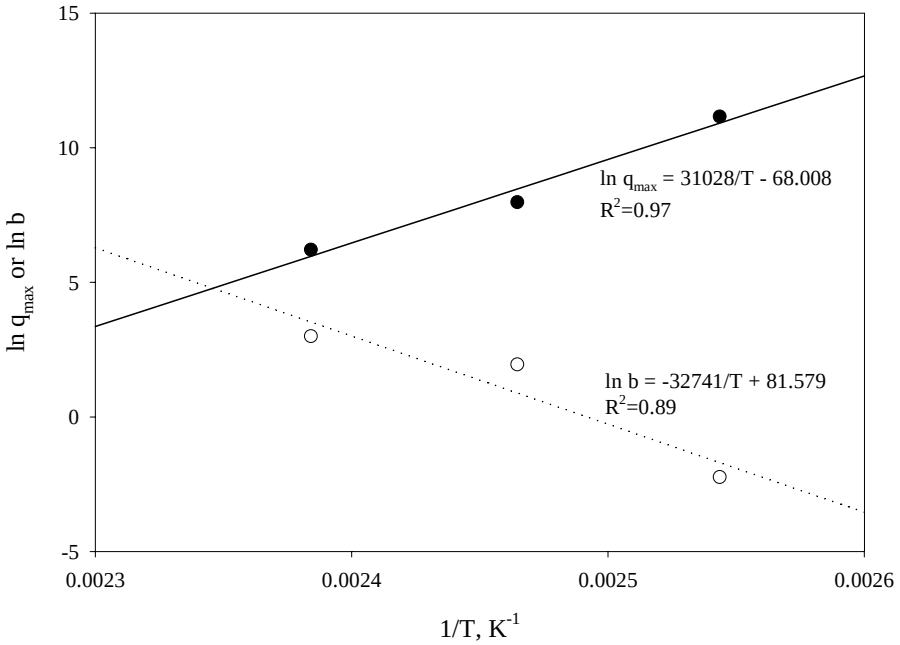

Figure 6. Variation of Langmuir isotherm parameters with temperature

Model Predictions

Figure 7 shows the model predictions for all the data sets (including the data sets used for model fitting) accounting for the variation of the isotherm coefficients with temperature. The model reasonably predicts the baghouse performance with the exception of a few data sets. Because data sets 1, 5, 17, and 23 did not have any carbon injection, the model predicted zero removal of mercury from the baghouse. However, 10% – 33% removal was observed experimentally, indicating that the fly ash itself or unburned carbon[21] may have contributed to mercury removal. In another case, because data sets 9 and 10 had the lowest carbon injection rates among all data sets, the model predicted modest removal efficiencies. However, the actual experimental removal efficiencies were negative. It would be expected that the removal efficiencies should at least be equal to the removal efficiencies associated with the fly ash (i.e., 10% – 33%). Reasons for this discrepancy are not clear at this time.

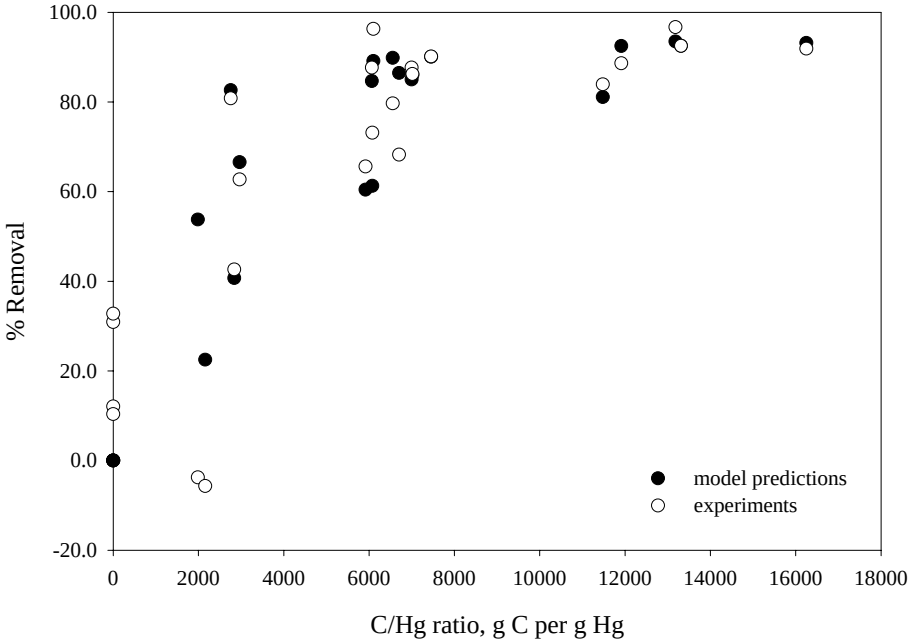

Figure 7. Effects of the carbon to mercury ratio on the average mercury removal for the NETL data sets

From Table 3 and Figure 6, it is clear that the temperature will significantly impact the removal of mercury from the baghouse. Another important process parameter that impacts the removal of mercury and is more easily controlled is the carbon dose. Figure 7 shows the carbon to mercury ratio for the experiments and the model. As expected, higher carbon doses result in greater removal of mercury in this system. The model predictions are also in agreement with the general trend of experimental data.

To further illustrate the effects of temperature and the carbon to mercury ratio, the effects of varying these parameters on the calculated average mercury removal is shown in Figure 8. The conditions for this figure are the same as the base conditions (Table 1) except that the isotherm parameters were varied with temperature using the equations in Figure 6. The range of temperature and C/Hg ratios are typical of the experimental conditions in the pilot scale tests and those that could be expected in full-scale operations. A decrease in the removal efficiency is observed at high temperatures because the adsorptive capacity at higher temperatures is lower. Increasing the carbon addition (hence increasing C/Hg ratio) will increase the removal efficiency at any temperature. The magnitude of the improvement in removal efficiency with C/Hg ratio is more pronounced at the higher temperatures where the carbon is more capacity limited. At lower temperatures, the system is more transfer limited and the removal efficiency is less sensitive to the mass of carbon added.

The impact of the cleaning cycle and the fraction of the bed cleaned per cycle is shown in Figure 9. Longer cleaning cycle results in a longer detention time of the particles on the fabric filter, which allows the carbon particles to adsorb more mercury from the bulk solution. This is different from a traditional fixed-bed adsorber because fresh, lightly loaded carbon particles are continuously being added to the influent of the growing bed where the mercury concentration is the highest. The mercury in the bulk phase decreases as it passes

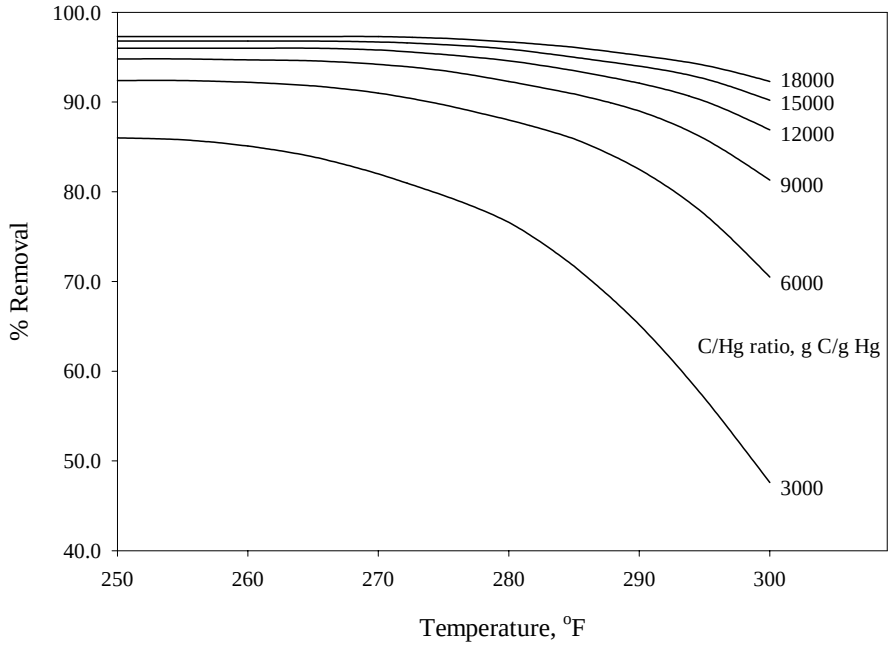

Figure 8. The effects of baghouse temperature and carbon dose (expressed as the carbon to mercury ratio) on mercury removal efficiency from the baghouse filter

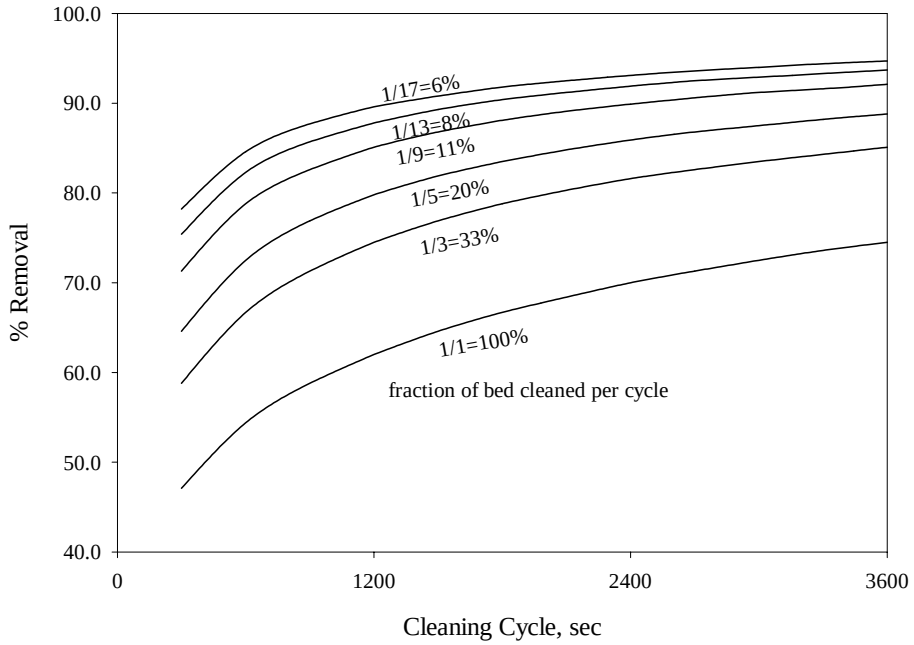

Figure 13. The effects of the cleaning cycle and the fraction of the baghouse cleaned per cycle on the calculated average mercury removal efficiency from the baghouse

through the bed and never achieves the breakthrough observed in a traditional fixed-bed adsorber. As the fabric filter is divided into different fractions for cleaning to maintain the pressure drop across the baghouse, lower fractional cleanings further allows the particles in the "uncleaned" section of the bed to uptake more mercury. The ideal case would be to have long cleaning cycles and low fractional bed cleaning, with the limits dictated by the allowable pressure drop across the baghouse filter.

CONCLUSIONS

Mercury removal in the activated carbon particle is modeled using a pore diffusion model with the Langmuir isotherm describing equilibrium between the gas phase and the carbon particle surface. Mercury removal in the duct is modeled using a plug flow system while mercury removal in the fabric filter is modeled using a growing-bed packed-bed approach. The presence of an external mass transfer boundary layer is accounted for in both stages. Advection, dispersion, and a periodic cleaning are accounted in the model of a growing packed bed on the fabric filter. Coordinate transformation is used to fix the spatial coordinates of the growing bed, making the model amenable to solving using orthogonal collocation techniques.

The key parameters that significantly impact the calculated average removal include the adsorption isotherm parameters and the carbon pore radius and tortuosity (or effectively, the pore diffusion coefficient). These parameters can be obtained from properly designed kinetic experiments. Critical baghouse operational parameters that will determine the calculated mercury removal include the C/Hg ratio, and the carbon particle size. The two-stage mathematical model was used to obtain Langmuir isotherm parameters for mercury on Norit Darco FGD sorbent at different temperatures. An Arrhenius relationship adequately quantified the variation of these parameters with temperature. The model reasonably described mercury removals measured on the pilot-scale system operated by the National Energy Technology Laboratory and was used to evaluate expected trends associated with a change in the process conditions (i.e., gas flowrates, mercury concentrations, temperature, carbon loading, etc.). Based on the model predictions, mercury removal in the duct appears to be limited and higher C/Hg ratio, lower operating temperature and longer cleaning cycle of the baghouse filter should be utilized to achieve higher mercury removal in this system.

ACKNOWLEDGEMENTS

This work was funded in part by the National Energy Technology Laboratory of the Department of Energy under Contract No. DE-AM26-99FT40463. The conclusions expressed in this manuscript are solely of the authors and do not necessarily reflect the views of the funding agency. Reference in this report to any specific commercial product, process, or service is to facilitate understanding and does not necessarily imply its endorsement or favoring by the United States Department of Energy. The authors also acknowledge Dr. Byung Kim from Ford Motor Company for valuable discussions on the numerical methods used in this study.

REFERENCES

1. Chen, S.; Rostam-Abadi, M.; Chang, R. *Proceedings of the 211th ACS National Meeting*, **1996**, New Orleans, LA, March 24-28, 41(1), 442-446.
2. Rostam-Abadi, M.; Chen, S.G.; Hsi, H-C; Rood, et al. *Proceedings of the First EPRI-DOE-EPA Combined Utility Air Pollution Control Symposium*, **1997**, Session B, Washinton DC, Aug 25-29.
3. Flora, J.R.V.; Vidic, R.D.; Liu, W.; Thurnau, R.C. *Journal of the Air & Waste Management Association*, **1998**, 48, 1051-1059.

4. Meserole, F.B.; Chang, R.; Carrey, T.R.; Machac, J.; Richardson, C.F. *J. Air & Waste Management Association*, **1999**, 49, 694-704.
5. Serre, S.D.; Gullett, B.K.; Ghorishi, S.B. *J. Air & Waste Management Association*, **2001**, 51, 733-741.
6. Scala, F. *Environmental Science and Technology*, **2001**, 35, 4367-4372.
7. Scala, F. *Environmental Science and Technology*, **2001**, 35, 4373-4378.
8. Flora, J.R.V., Hargis, R.A., O'Dowd, W.J., Pennline, H.W. and Vidic, R.D. *J. AWMA*, submitted for publication, 2002.
9. Finlayson, B.A. *Nonlinear Analysis in Chemical Engineering*, McGraw-Hill, New York, **1980**.
10. Brenan, K.E.; Campbell, S.L.; Petzold, L.R. *Numerical Solution of Initial-Value Problems in Differential-Algebraic Equations*, North-Holland, New York, **1989**.
11. Crank, J. *Free and Moving Boundary Problems*, Oxford University Press, New York, **1984.**
12. Knudsen, J.G.; Hottel, H.C.; Sarofim, A.F.; Wankat, P.C.; Knaebel, K.S. *Section 5 – Heat and Mass Transfer*, In *Perry's Chemical Engineer's Handbook, 7th Ed.*, Green, D.W. and Maloney, J.O. (editors), McGraw-Hill, New York, **1997**.
13. Cussler, E.L. *Diffusion: Mass Transfer in Fluid Systems*, Cambridge University Press, New York, **1984.**
14. Ruthven, D.M. *Principles of Adsorption and Adsorption Processes*, John Wiley and Sons, Inc., **1984.**
15. Wark, K.; Warner, C.F. *Air Pollution: Its Origin and Control*, Harper and Row Publishers, New York, **1981**.
16. Wakao, N.; Funazkri, T. *Chemical Engineering Science*, **1978**, 33, 1375-1384.
17. Hsi, H.-C.; Chen, S.; Rostam-Abadi, M.; Rood, M.J.; Richardson, C.F.; Carey, T.R.; Chang, R.L. *Energy and Fuels*, **1998**, 12, 1061-1070.
18. Yang, R.T. *Gas Separation by Adsorption Processes*, Butterworth's Inc., Boston, **1987**.
19. Bush, P.V.; Snyder, T.R.; Chang, R.L. *Journal of the Air Pollution Control Association*, **1989**, 39(2), 228-237.
20. Hargis, R.A.; O'Dowd, W.J.; Pennline, H.W. *Proceedings of the 17th Annual Pittsburgh Coal Conference*, **2000**, Pittsburgh, PA, September 11-14.
21. Hargis, R.A.; O'Dowd, W.J.; Pennline, H.W. *Proceedings of the 26th International Technical Conference on Coal Utilization and Fuel Systems*, **2001**, Clearwater, FL, March 5-8.
22. Code of Federal Regulations, 40CFR61, Appendix B, Method 101A, 1996.
23. ASTM, Standard Test Method for Elemental, Oxidized, Particle-Bound, and Total Mercury in Flue Gas Generated from Coal-Fired Stationary Sources (Ontario-Hydro Method), Draft, 1998
24. Goffe, W.L.; Ferrier, G.D.; Rogers, J. *J. of Econometrics*, **1994**, 60(1/2), 65-100.
25. Livengood, C.D.; Huang, H.S.; Wu, J.M. *Proceedings of the 87th Annual Meeting of the Air & Waste Management Association*, **1994**, preprint, 14 p.
26. Karatza, D.; Lancia, A.; Musmarra, D.; Pepe, F.; Volpicelli, G. *Combustion Science and Technology*, **1996**, 112, 163-174.
27. Karatza, D.; Lancia, A.; Musmarra, D. *Environmental Science and Technology*, **1998**, 32(24), 3999-4004.